Nonperturbative β function and effective radiative corrections

Ralf Hofmann

ITP Universität Heidelberg

2nd Winter Workshop on Non-Perturbative Quantum Field Theory
5-7 October 2011
Sophia-Antipolis (France)

7 October 2011

Table of Contents I

Trace anomaly for $\theta_{\mu\nu}$ and nonperturbative β function
- Historical remarks and objective
- Trace anomaly, effectively
- Running coupling: temperature vs. resolution
- Evaluation of gluon condensate
- Nonperturbative gauge-coupling evolution

Effective radiative correction
- Pressure: 2-loops and 3-loops
- Polarization tensor of massless mode
  - Transverse dispersion relation
  - Black-body spectrum
  - Longitudinal dispersion relation
- Monopole properties from a 2-loop correction to pressure

Trace anomaly for $\theta_{\mu\nu} \equiv 2\,\mathrm{tr}\,\left(-F_{\mu\lambda}F^{\lambda}_{\nu} + \frac{1}{4}g_{\mu\nu}F^{\kappa\lambda}F_{\kappa\lambda}\right)$

- to any loop order in PT, trace anomaly:

$$\theta_{\mu\mu} = \frac{\beta(g)}{2g}\,F^{a}_{\mu\nu}F^{a}_{\mu\nu} \quad (*)$$

[Collins, A. Duncan, and Joglekar 1977; Fujikawa 1980]

- to any loop order in PT and nonperturbatively (path integral), chiral anomaly:

$$\partial_{\mu}j^{5}_{\mu} = \frac{1}{32\pi^{2}}\,F^{a}_{\mu\nu}\tilde{F}^{a}_{\mu\nu}\,.$$

[Adler, Adler and Bardeen 1969; Bell and Jackiw 1969; Fujikawa 1979,1980]

- in constrast to trace anomaly **chiral anomaly not renormalized** and topologically saturated

Trace anomaly, effectively

- **idea:** use operator identity (*) to extract $\beta(g)$ and thus $g(T)$ from (effective) knowledge of $\langle\theta_{\mu\mu}\rangle_T$ and $\left\langle F^a_{\mu\nu}F^a_{\mu\nu}\right\rangle_T$ in deconfining SU(2) and SU(3) Yang-Mills thermodynamics [Giacosa and RH 2008]
- on one-loop level, one has in effective theory:

$$\begin{aligned}\langle\theta_{\mu\mu}\rangle_T &= \rho - 3p \\ &= T^4\left(2\frac{\pi^2}{30} + \frac{3}{\pi^2}\int_0^\infty dx \frac{x^2\sqrt{x^2+a^2}}{e^{\sqrt{x^2+a^2}}-1} + \frac{2(2\pi)^4}{\lambda^3}\right. \\ &\quad \left. -6\frac{\pi^2}{90} + \frac{3}{\pi^2}\int_0^\infty x^2 dx \ln\left(1-e^{-\sqrt{x^2+a^2}}\right) + 6\frac{(2\pi)^4}{\lambda^3}\right),\end{aligned}$$

where $a \equiv \frac{2e|\phi|}{T}$, $|\phi| = \sqrt{\frac{\Lambda^3}{2\pi T}}$, $\lambda \equiv \frac{2\pi T}{\Lambda}$, and $e \equiv \sqrt{8\pi}$ **almost everywhere** in deconfining phase.

Trace anomaly, effectively

- use of one-loop approximation justified by **hierarchically suppressed, effective radiative corrections** (later)
- going from **fundamental** to **effective** fields $\Rightarrow$ fundamental field strength $F_{\mu\nu}$ suffers wave-function renormalization (**fundamental** radiative corrections); thus

$$\langle \mathcal{L}_{\mathrm{YM}} \rangle_T = \frac{1}{4} \left\langle F^a_{\mu\nu} F^{a,\mu\nu} \right\rangle_T = f^2(g) \langle \mathcal{L}_{\text{dec-eff}} \rangle_T = f^2(g) \rho_{gs}$$

where $\rho_{gs} = 4\pi\Lambda^3 T$, and real function $f(g)$ to be determined later.

(effective excitations do not contribute to average over action density!)

Running coupling: temperature vs. resolution

- in general: $\beta(g) \equiv \mu\, \partial_\mu g$.
- since (derivation of effective theory) a *natural* value for μ is
  $\mu = |\phi| = \sqrt{\frac{\Lambda^3}{2\pi T}} \Rightarrow$
  $\beta(g) \equiv |\phi|\, \partial_{|\phi|} g = -2T\, \partial_T g \equiv -2\beta_T(g)$
- **moreover:** (*) recast as $h(\lambda) \equiv \frac{\rho - 3p}{4\rho_{gs}} = -\frac{\beta_T(g)}{g} f^2(g)$,
  where perturbatively $\beta_T(g) = -bg^3$ ($b = \frac{11N}{48\pi^2}$, $N = 2, 3$) at one loop
  But:

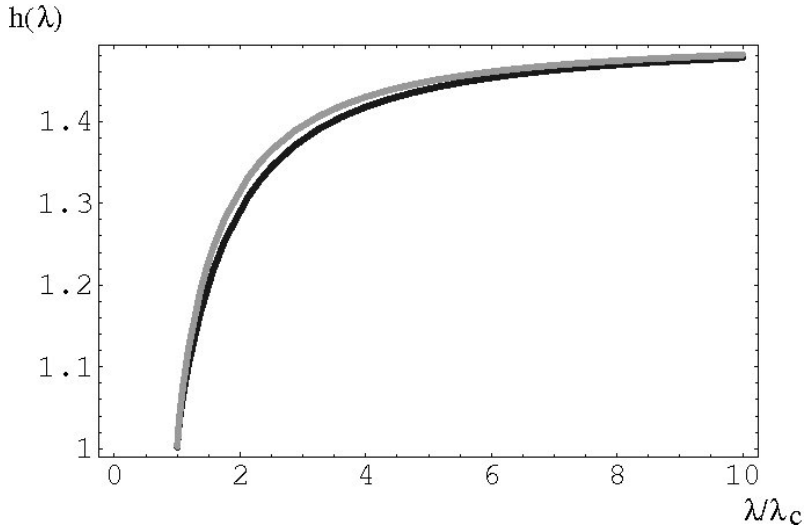

Function $h(\lambda)$ for SU(2) (gray) and SU(3) (black).

Running coupling: temperature vs. resolution

$\Rightarrow$

β function for running of g in dependence of T **negative**.

$\Rightarrow$

β function for running of g in dependence of resolution ($\mu = |\phi|$) **positive**.

Evaluation of gluon condensate

- **assumption:** in

$$h(\lambda) \equiv \frac{\rho - 3p}{4\rho_{gs}} = -\frac{\beta_T(g)}{g} f^2(g)$$

all nonperturbative and higher-loop effects contributing to h reside in $\beta_T(g)$
$\Rightarrow f^2(g)$ can be determined from high-T asymptotics
(one-loop expression for $\beta_T(g)$ and $h_\infty = \frac{3}{2}$)
$\Rightarrow f(g) = \sqrt{\frac{3}{2b}}\,\frac{1}{g}$.

- **gluon condensate:** $\frac{1}{4}\left\langle F^a_{\mu\nu} F^{a,\mu\nu} \right\rangle_T = 4\pi\Lambda^3 T\,\frac{3}{2b}\,\frac{1}{g^2}$, where g is solution to

$$\beta_T(g) = -\frac{2}{3}\, b\, h(\lambda) g^3 \Leftrightarrow \partial_\lambda g = -\frac{2}{3}\, b\, \frac{h(\lambda)}{\lambda} g^3 \,.$$

Nonperturbative gauge-coupling evolution

- **without calculation:** evolution equation

$$\beta_T(g) = -\frac{2}{3}\, b\, h(\lambda) g^3 \Leftrightarrow \partial_\lambda g = -\frac{2}{3}\, b\, \frac{h(\lambda)}{\lambda} g^3 \,.$$

$\Rightarrow$ since $h(\lambda) \leq \frac{3}{2}$ negative slope nonperturbatively screened
$\Rightarrow$ nonpert. Landau pole at lower T than pert. one
(Recall: $T_L = T_0 \exp\left(-\frac{1}{2bg_0^2}\right)$.)

- boundary conditions to evolution of g:
  - $e(\lambda)$ logarithmic pole at $\lambda_c = 13.87$
  - $g(\lambda)$ nonperturbative Landau pole at $\lambda_c = 13.87$
  - $g_P(\lambda)$ matches $g(\lambda)$ at high λ, say, at $\lambda = 10\,\lambda_c$

Nonperturbative gauge-coupling evolution:

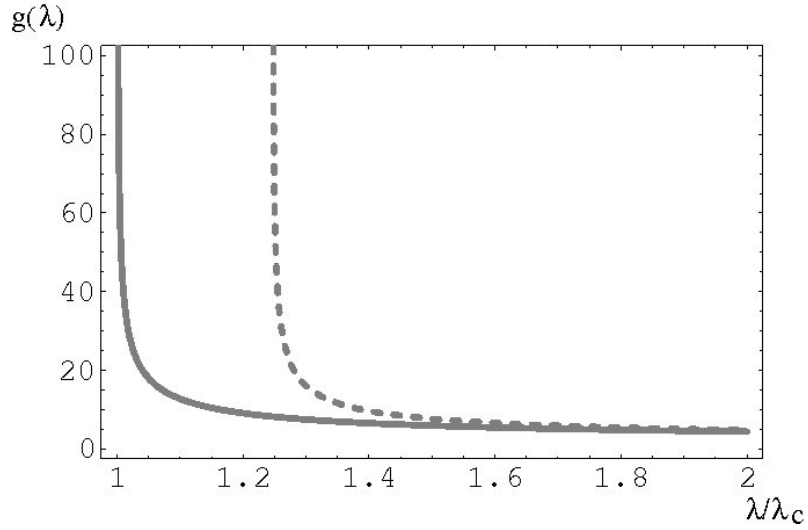

$g(\lambda)$ and $g_P(\lambda)$ for SU(2).

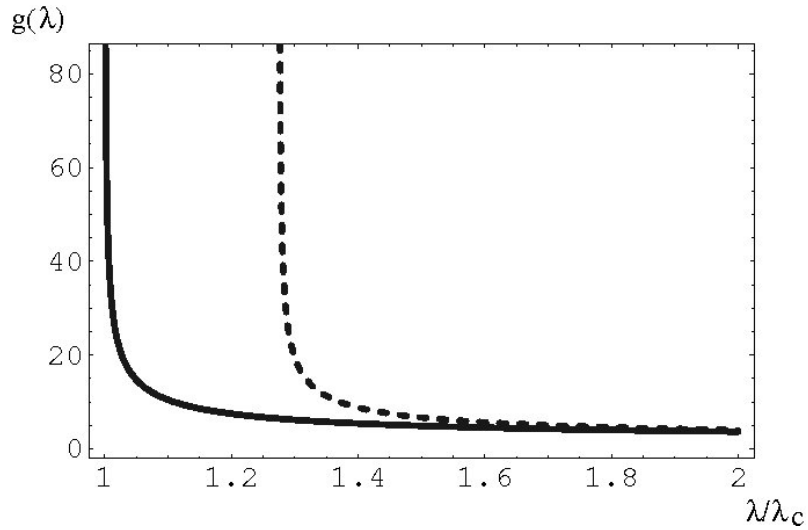

$g(\lambda)$ and $g_P(\lambda)$ for SU(3).

Effective radiative corrections: 2-loop diagrams

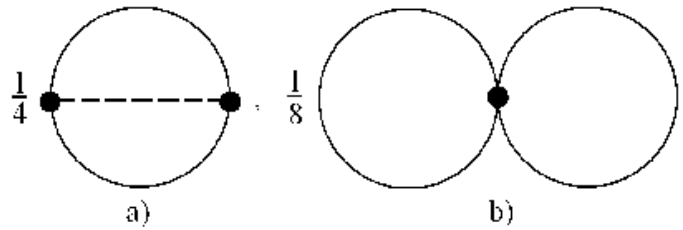

solid (dashed) lines $\leftrightarrow$ massive (massless) modes

$$\begin{aligned}
\Delta P_a &= \frac{1}{8\mathrm{i}} \int \frac{\mathrm{d}^4 p\, \mathrm{d}^4 k}{(2\pi)^8} \Gamma^{\lambda\mu\nu}_{[3]abc}(p,k,-p,-k) \Gamma^{\rho\delta\tau}_{[3]rst}(-p,-k,p+k) \\
&\quad \times D_{\lambda\rho,ar}(p) D_{\mu\rho,bs}(k) D_{\nu\tau,ct}(-p,-k), \\
\Delta P_b &= \frac{1}{8\mathrm{i}} \int \frac{d^4 p\, d^4 k}{(2\pi)^8} \Gamma^{\mu\nu\rho\delta}_{[4]abcd} D_{\mu\nu,ab}(p) D_{\rho\delta,cd}(k)
\end{aligned}$$

plus constraints: on-shellness of massive modes, $|(p+k)^2| \leq |\phi|^2$ in diagram (b)

2-loop diagrams, constraints

- Potentially noncompact independent loop variables for 2-loop diag are $(p_0, |\mathbf{p}|)$ and $(k_0, |\mathbf{k}|)$.
  Number of potentially noncompact independent loop variables $\tilde{K} = 4$
- The constraints for 2-loop diagrames are
  – on-shellness: $p^2 = k^2 = 4e^2|\phi|^2$
  – compositeness constraints:

$$\left| 4e^2 \pm \sqrt{x_1^2 + 4e^2}\sqrt{x_2^2 + 4e^2} - x_1 x_2 z_{12} \right| \leq \frac{1}{2}\,,$$

  where $x_1 \equiv \frac{|\mathbf{p}|}{|\phi|}$ and $x_2 \equiv \frac{|\mathbf{k}|}{|\phi|}$
- For 2-loop, we have a total number of constraints

$$K = 1 + 2 = 3$$

- Thus for the 2-loop case: more noncompact loop variables than constraints: $\tilde{K} > K$
- $\Rightarrow$ noncompact integration region

selected 2-loop diag. (b)

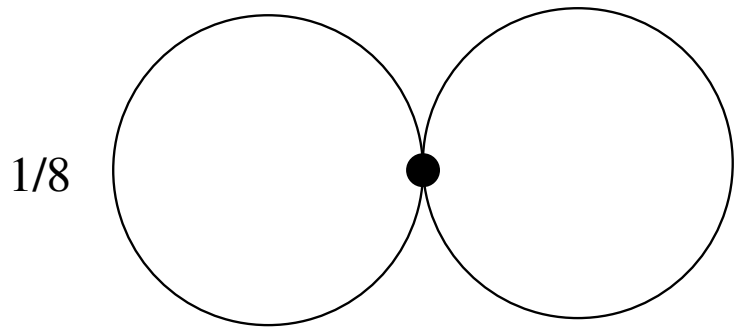

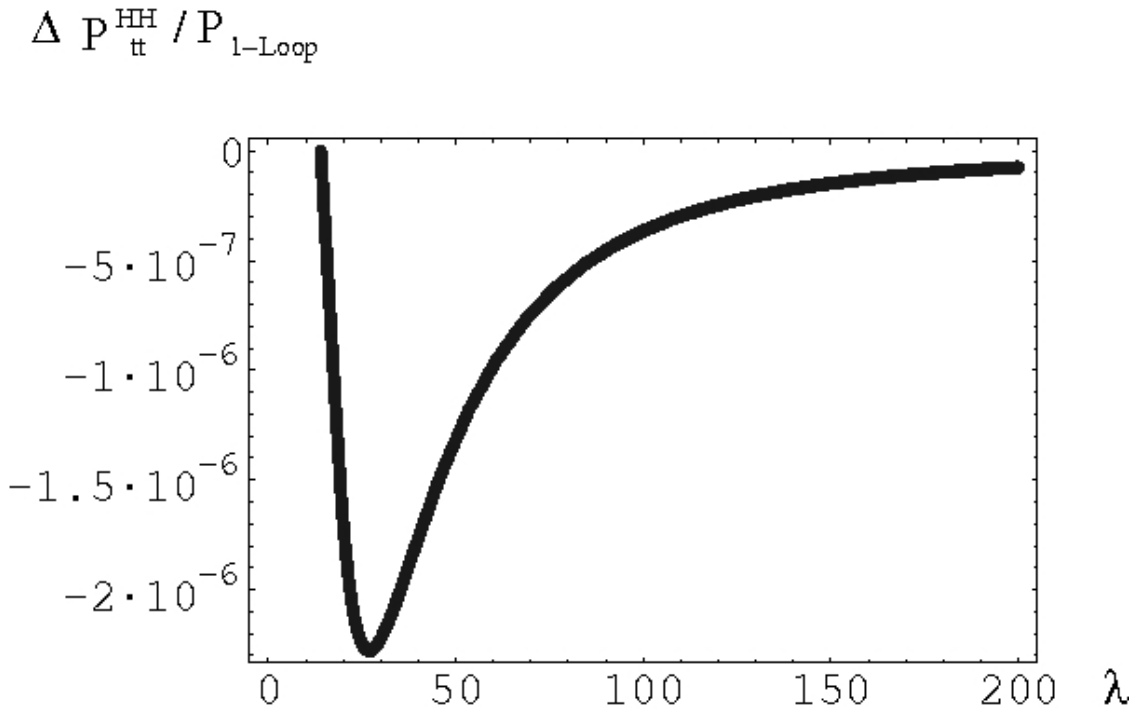

Effective radiative corrections: 3-loop diagrams

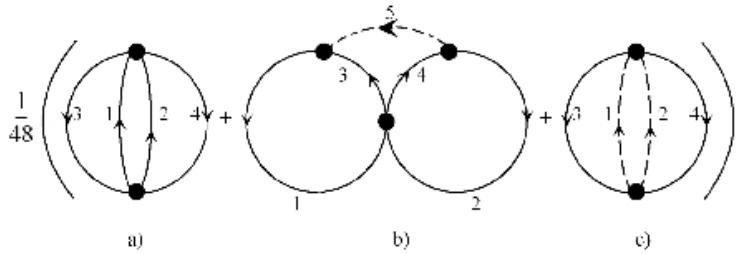

Ir. 3-loop diagrams: Solid (dashed) lines are associated with the propagators of massive (massless) modes

$$\Delta P_a = \frac{1}{48} \int \frac{\mathrm{d}^4p_1\mathrm{d}^4p_2\mathrm{d}^4p_3}{(2\pi)^4(2\pi)^4(2\pi)^4} \Gamma^{\mu\nu\rho\sigma}_{[4]abcd} \Gamma^{\bar\mu\bar\nu\bar\rho\bar\sigma}_{[4]\bar a\bar b\bar c\bar d} \times D_{\rho\bar\rho,c\bar c}(p_1) D_{\sigma\bar\sigma,d\bar d}(p_2) D_{\mu\bar\mu,a\bar a}(p_3) D_{\nu\bar\nu,b\bar b}(p_4),$$

$$\Delta P_b = \frac{1}{48} \int \frac{\mathrm{d}^4p_1\mathrm{d}^4p_2\mathrm{d}^4p_3}{(2\pi)^4(2\pi)^4(2\pi)^4} \Gamma^{\alpha\beta\gamma\lambda}_{[4]hijk} \Gamma^{\mu\nu\rho}_{[3]abc} \Gamma^{\bar\mu\bar\nu\bar\rho}_{[3]\bar a\bar b\bar c} D_{\mu\alpha,ah}(p_1) \times D_{\bar\mu\beta,\bar a i}(p_2) D_{\gamma\rho,jc}(p_3) D_{\lambda\bar\rho,k\bar c}(p_4) D_{\mu\bar\nu,b\bar b}(p_5)$$

$$\Delta P_c = \frac{1}{48} \int \frac{\mathrm{d}^4p_1\mathrm{d}^4p_2\mathrm{d}^4p_3}{(2\pi)^4(2\pi)^4(2\pi)^4} \Gamma^{\mu\nu\rho\sigma}_{[4]abcd} \Gamma^{\bar\mu\bar\nu\bar\rho\bar\sigma}_{[4]\bar a\bar b\bar c\bar d} D_{\rho\bar\rho,c\bar c}(p_1) \times D_{\sigma\bar\sigma,d\bar d}(p_2) D_{\mu\bar\mu,a\bar a}(p_3) D_{\nu\bar\nu,b\bar b}(p_4)$$

3-loop diagrams, general constraints

- Potentially noncompact independent loop variables for ir. 3-loop diags are $(p_0, |\mathbf{p}|)_i$ for $i = 1, 2, 3$.
  Number of potentially noncompact independent loop variables

$$\tilde{K} = 6$$

- The compositeness constrains for ir. 3-loop diags. are

$$\begin{aligned} |(p_1 + p_2)^2| &\leq |\phi|^2 \quad (s \text{ channel}) \\ |(p_3 - p_1)^2| &\leq |\phi|^2 \quad (t \text{ channel}) \\ |(p_2 - p_3)^2| &\leq |\phi|^2 \quad (u \text{ channel}) \end{aligned}$$

- Additional constraints depend on the number of massless and massive propagators in each individual ir. 3-loop diag.

Constraints and compactness: ir. 3-loop diag. (a) and (b)

- We have 3 compositeness constraints due to the s-, t-, u-channels
- In addition to the compositeness constraints, we have the on-shellness conditions:

$$p_1^2 = m^2, \quad p_2^2 = m^2, \quad p_3^2 = m^2, \quad p_4^2 = (p_1 + p_2 - p_3)^2 = m^2$$

- The max. off-shellness of the massless mode in diag. (b) is automatically satisfied by the t-channel due to momentum conservation, $p_5 = p_1 - p_3$
- The total number of constraints for diag. (a) and (b) is

$$K = 3 + 4 = 7$$

- Thus for ir. 3-loop diag. (a) and (b) we have

$$\tilde{K} = 6 < 7 = K$$

$\Rightarrow$ Compact integration region

Constraints and compactness: ir. 3-loop diag. (c)

- As before, we have 3 compositeness constraints over the s-, t-, u-channels
- In addition to the compositeness constraints, the on-shellness relations for the massive modes in diag. (c)

$$p_3^2 = m^2, \quad p_4^2 = (p_1 + p_2 - p_3)^2 = m^2$$

- For diag. (c), we also have the following constraints due to the max. off-shellness

$$|p_1^2| \leq |\phi|^2, \quad |p_2^2| \leq |\phi|^2$$

- The above constraints yield for diag. (c)

$$K = 3 + 4 = 7$$

- Thus for all ir. 3-loop diag. $K = 3 + 4 = 7$ and

$$\tilde{K} < K$$

$\Rightarrow$ Compact or empty integration region

results: ir. 3-loop diag. (a) and (b)

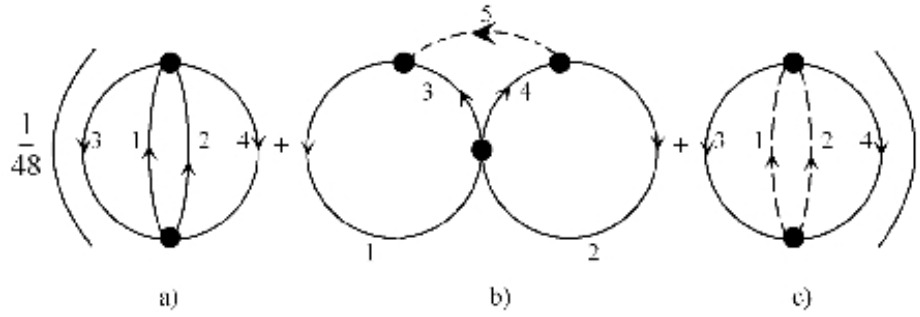

$> |\Delta P_A| / P_{1-loop}$

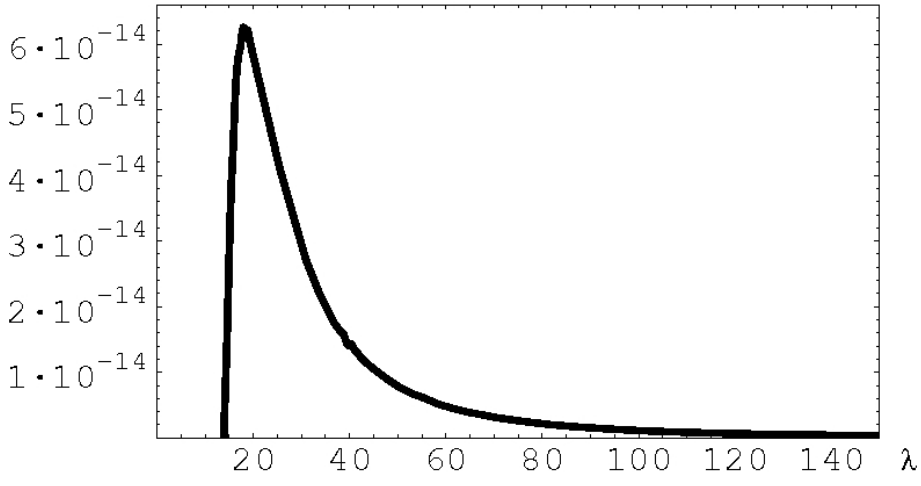

$> |\Delta P_B| / P_{1-loop}$

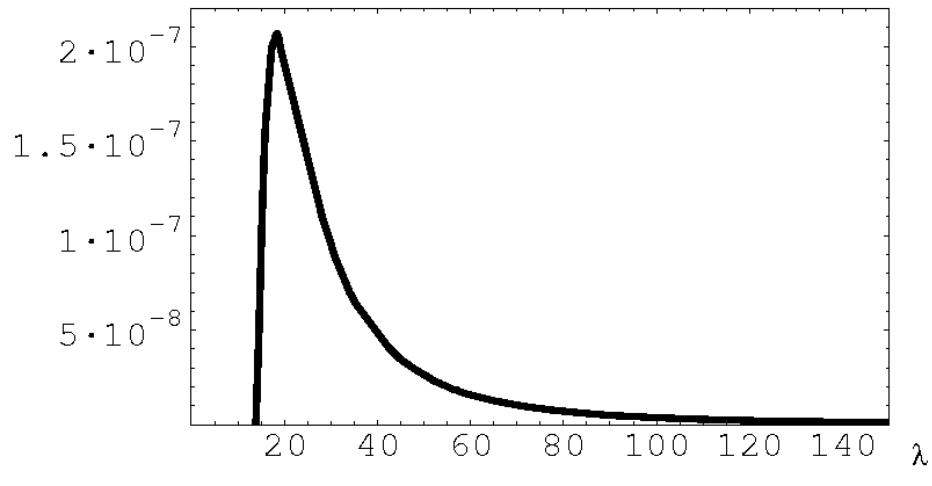

Hierarchy between 2-loop and 3-loop corrections

- Ir. 3-loop integrations generate **hierarchically suppressed contributions** to the pressure over the 2-loop contributions:

$$\frac{P_{\text{2-loop}}}{P_{\text{1-loop}}} \leq 10^{-2}$$

$$\frac{P_{\text{3-loop}}}{P_{\text{1-loop}}} \leq 10^{-5} \frac{P_{\text{2-loop}}}{P_{\text{1-loop}}} = 10^{-7}$$

- Ir. 3-loop integrations are **either compact** (ir. diags. (a)-(b)) **or empty** (ir. diag. (c)) whereas 2-loop integrations are noncompact
- The most striking difference between 2-loop and 3-loop corrections: the contribution from the ir. 3-loop diag. (c) is vanishing; no 2-loop diagram has this property

Relation between pressure and polarization tensor

The polarization tensor is a sum over connected bubble diags. with one internal line of momentum p cut, such that the diag. remains connected, and the two so-obtained external lines amputated

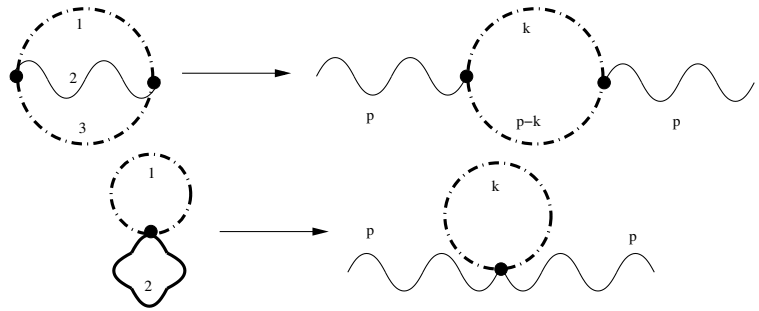

Consequences:

- The hierarchical suppression of 3-loop compared to 2-loop justifies the **calculation of the polarization tensor on 1-loop level**.
- The vanishing of a connected bubble diag. due to a zero-measure support for its loop-momenta integrations implies that the associated contribution to a polarization tensor is also nil.

Effective radiative corrections: Pol. tensor massless mode

modified dispersion laws: transverse and longitudinal parts (real time)

$$D^{TLM}_{\mu\nu,ab}(p_t) = -\delta_{a3}\delta_{b3}P^T_{\mu\nu}\left[\frac{\mathrm{i}}{p_t^2 - G} + 2\pi\delta(p_t^2 - G)\, n_B(|p_{0,t}|/T)\right]$$

$$D^{TLM}_{\mu\nu,ab}(p_l) = \delta_{a3}\delta_{b3}u_\mu u_\nu\left[\frac{p_l^2}{\mathbf{p}_l^2}\frac{\mathrm{i}}{p_l^2 - F} - 2\pi\delta(p_l^2 - F)\, n_B(|p_{0,l}|/T)\right]$$

Poles yield dispersion relations ($p_0 = \omega + \mathrm{i}\gamma$, assume $\gamma \ll \omega$):

$$\omega_t^2(\mathbf{p}_t) = \mathbf{p}_t^2 + \mathrm{Re}G(\omega(\mathbf{p}_t), \mathbf{p}_t) \qquad \omega_l^2(\mathbf{p}_l) = \mathbf{p}_l^2 + \mathrm{Re}F(\omega_L(\mathbf{p}_l), \mathbf{p}_l)$$

$$\gamma(\mathbf{p}_t) = -\mathrm{Im}G(\omega(\mathbf{p}_t), \mathbf{p}_t)/2\omega \qquad \gamma_l(\mathbf{p}_l) = -\mathrm{Im}F(\omega_l(\mathbf{p}_l), \mathbf{p}_l)/2\omega_l$$

Pol. tensor massless mode cntd.

Chosing $\mathbf{p} \parallel e_3$:

$$G(p_0, \mathbf{p}) = \Sigma^{11} = \Sigma^{22}$$

$$F(p_0, \mathbf{p}) = \left(1 - \frac{p_0^2}{p^2}\right)^{-1} \Sigma^{00}$$

$\Sigma^{\mu\nu}$ sum of two diagrams:

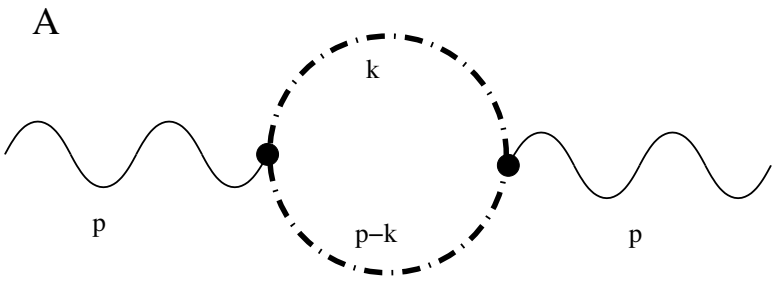

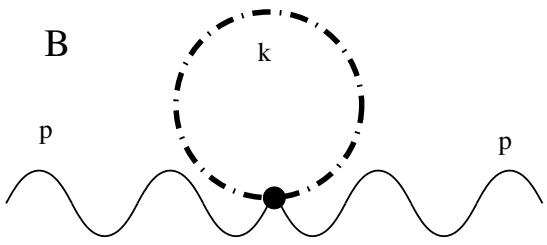

Purely imaginary: $\Rightarrow$ yields γ

One-loop level sufficient!

Purely real: $\Rightarrow$ yields dispersion relation

Full calculation of G

Gap equation:

$$\begin{aligned}\mathrm{Re}G(p_0,\mathbf{p}) = 8\pi e^2 \int_{|(p+k)^2|\leq|\phi|^2} &\left[-\left(3-\frac{k^2}{m^2}\right)+\frac{k^1k^1}{m^2}\right] \\ &\times n_{\mathrm{B}}\left(|k_0|/T\right)\delta\left(k^2-m^2\right)\left.\frac{\mathrm{d}^4k}{(2\pi)^4}\right|_{p^2=G} \\ &\equiv H(T,\mathbf{p},G)\end{aligned}$$

Via δ-function, integration over k_0 yields $k_0 \to \pm\sqrt{\mathbf{k}^2+m^2}$.
With $p_0 = \pm\sqrt{\mathbf{p}^2+G(p_0,\mathbf{p})}$ and $\mathbf{p} \parallel \mathbf{e}_3$ constraint reads

$$\left|G+2\left(\pm\sqrt{\mathbf{p}^2+G}\sqrt{\mathbf{k}^2+m^2}-pk_3\right)+m^2\right| \leq |\phi|^2$$

Selfconsistent result for G, real part

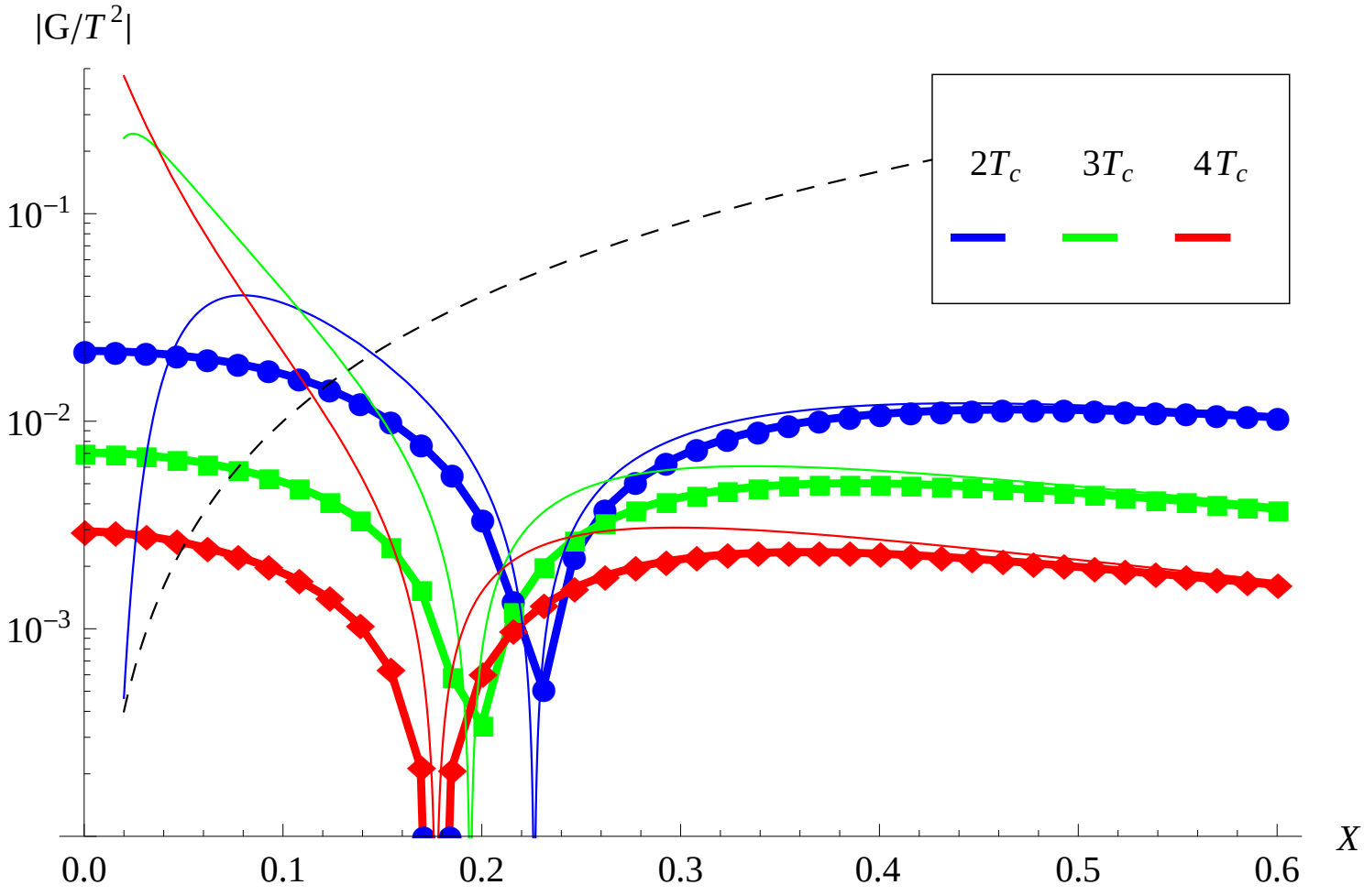

Selfconsistent result for G, real part

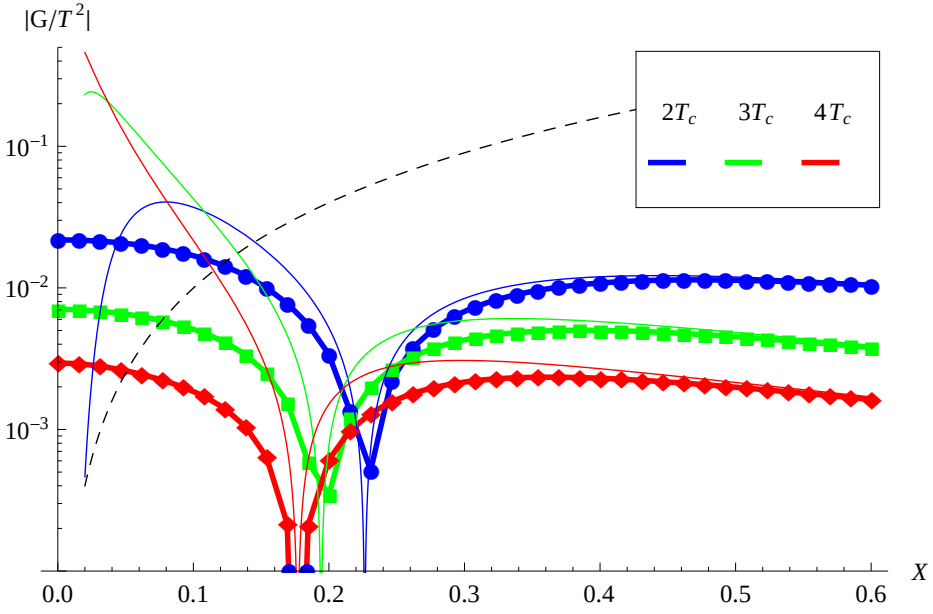

- $X \gtrsim 0.2$: $G < 0$ (anti-screening)
- Dip: $G = 0$
- $X \lesssim 0.2$: $G > 0$ (screening)

Comparison with approximate result:

- Zeros of G agree (must be)
- For $X \gtrsim 0.2$, approximate agrees with selfconsistent result (expected)
- Results different when $G \gtrsim X^2$ (not suprising)

Selfconsistent result for G, imaginary part

Imaginary part: $\mathrm{Im}G \propto$ 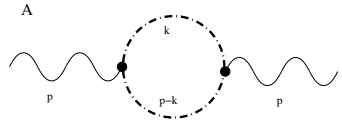

At left vertex: particle with mass $\sqrt{G}$ decaying into two on-shell particles with mass m only possible if

$$\frac{G}{T^2} \geq 4\frac{m^2}{T^2} = 64\pi^2\frac{e^2}{\lambda^3} \tag{1}$$

- $G \leq 0$: condition (1) never satisfied
- $G > 0$:

$$\frac{G(X=0,T)}{T^2} \propto \frac{1}{\lambda^3} \ll 64\pi^2\frac{e^2}{\lambda^3} \sim 5\times 10^4/\lambda^3$$

  condition (1) never satisfied

Diagram A $= 0$, hence no imaginary part of G, hence $\gamma = 0$ and assumption $\gamma \ll \omega$ satisfied trivially.

Black-body spectra for $T \sim T_c$

modification of U(1) by screening function G:

[Schwarz, Hofmann, Giacosa 2006; Ludescher and Hofmann 2008]

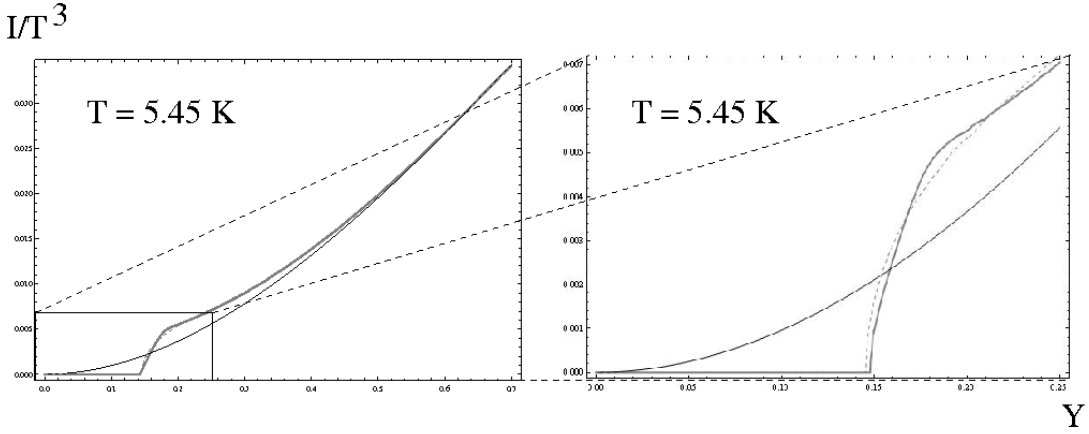

postulating SU(2) as theory for photon propagation:

- $T_c = 2.725\,\mathrm{K}$, UEGE confirmed by Arcade2 [Hofmann 2009]
- measurable gap in spectral radiance [Falquez, Hofmann, Baumbach 2010]

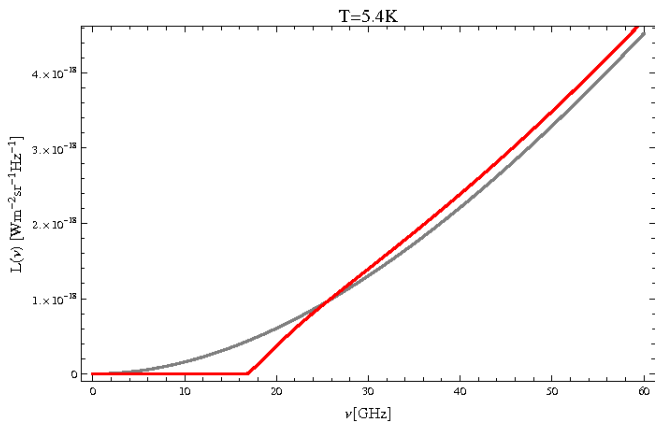

Full calculation of F

Assume $F \in \mathbb{R}$ (turns out to be selfconsistent)

Apply Feynman rules to $\mathbf{p}^2 = \mathrm{Re}\Sigma^{00} =$ 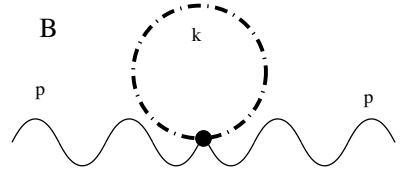

yields gap equation:

$$\mathbf{p}^2 = \Sigma_{\mathrm{B}}^{00}(p) = 8\pi e^2 \int_{|(p+k)^2| \leq |\phi|^2} \left[\left(3 - \frac{k^2}{m^2} \right) + \frac{k^0 k^0}{m^2} \right] \times n_{\mathrm{B}} \left(|k_0| / T \right) \delta \left(k^2 - m^2 \right) \frac{\mathrm{d}^4 k}{(2\pi)^4} \Bigg|_{p^2 = F} \quad (2)$$

Strategy to find F similar to that of finding G

[Falquez, Hofmann, Baumbach 2010].

Selfconsistent result for F

$$Y_l \equiv \frac{\omega_l(\mathbf{p}_l, T)}{T} = \sqrt{\frac{F(p_l^2, T)}{T^2} + \frac{\mathbf{p}_l^2}{T^2}},\ X \equiv |\mathbf{p}_l|/T$$

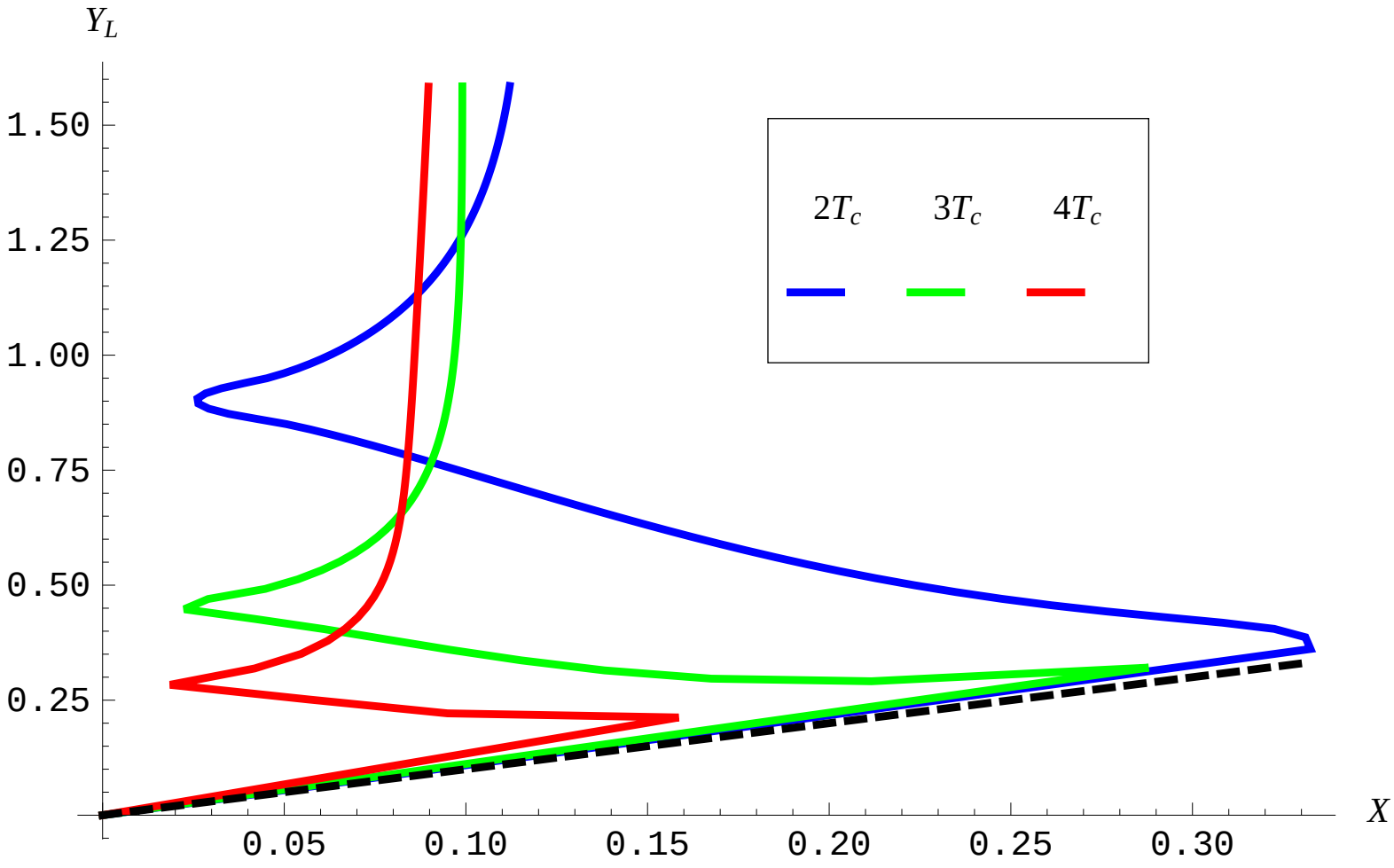

Selfconsistent result for F

$$Y_l \equiv \frac{\omega_l(\mathbf{p}_l, T)}{T} = \sqrt{\frac{F(p_l^2, T)}{T^2} + \frac{\mathbf{p}_l^2}{T^2}},\ X \equiv |\mathbf{p}_l|/T$$

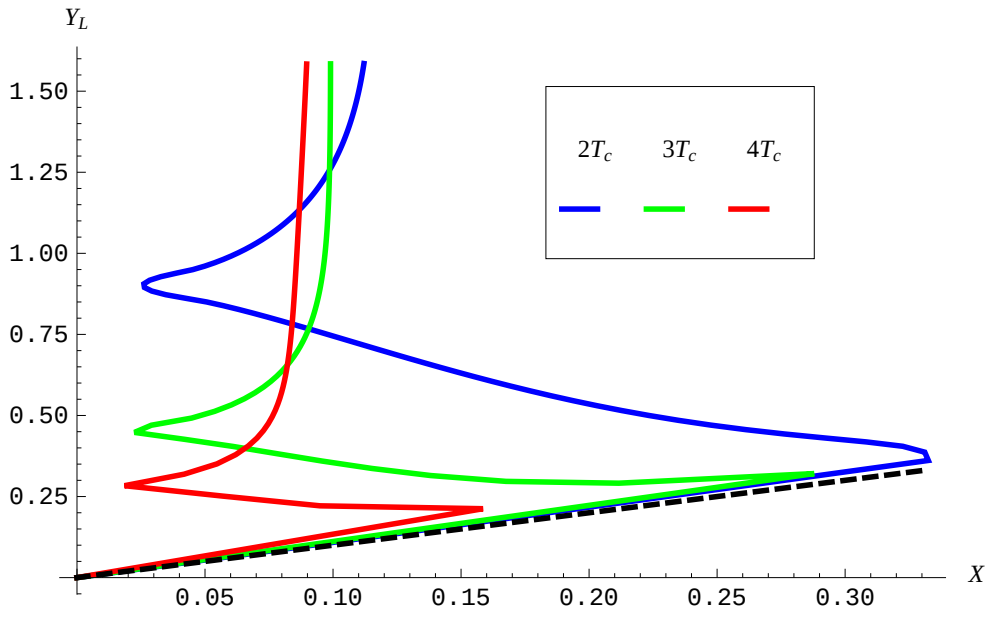

- 3 branches
- Y_L defined only for $X \lesssim 0.34$
- superluminal group velocity

Selfconsistent result for F, interpretation

charge-density waves $\leftrightarrow$ interpretation in terms of magnetic monopoles

[Falquez, Hofmann, Baumbach 2011]

- longitudinal modes due to charge density waves
- light like propagation:
  - stable (yet unresolved) monopoles released by large holonomy caloron dissociation [Diakonov et al. 2004]
  - density disturbance can only be propagated by radiation field, which propagates at the speed of light

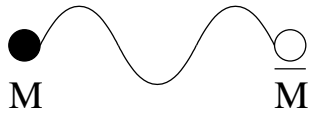

- superluminal propagation:
  - unstable monopoles contained in small holonomy caloron
  - extended calorons provide instantaneous correlation between monopoles, leading to superluminal propagation

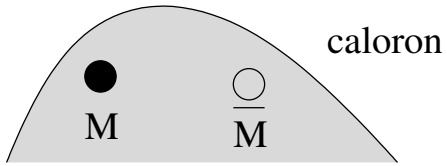

A particular 2-loop correction to pressure

- "Bubble diagrams" yield pressure
- For $T \gg T_c$ only relevant diagram:

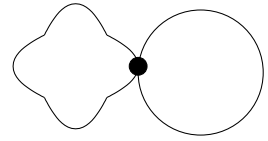

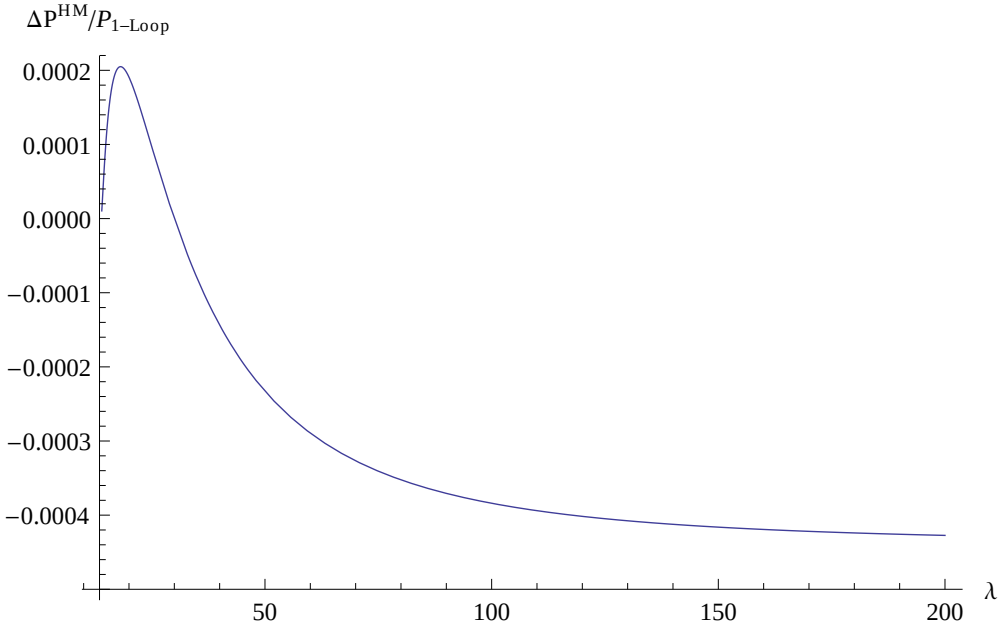

- $\Delta P \propto -4 \times 10^{-4} T^4$
- Temperature of TLM gas reduced!

Monopole properties

Explanation

Energy used to break up calorons, creating monopole anti-monopole pairs

[Schwarz et al. 2006; Ludescher et al. 2008]

Detailed analysis shows [Ludescher et al. 2008]:

- average monopole-antimonopole distance $\bar{d} < |\phi|^{-1}$
  $\Rightarrow$ monopoles unresolved in effective theory
- screening length l_s due to small-holonomy calorons: $l_s = 3.3\bar{d}$
  $\Rightarrow$ magnetic flux of monopole and antimonopole cancel (no area law for spatial Wilson loop)

Summary

Summary:

- computation of nonperturbative running of **fundamental** coupling g:
  definition via trace anomaly, β function **positive** w.r.t. running **resolution**, β function **negative** w.r.t. running **temperature**, mild screening of Landau pole
- radiative corrections: pressure at 2-loops and 3-loops; large hierarchy
- radiative corrections: polarization tensor of massless mode
- radiative corrections: black-body anomaly
- radiative corrections: monopole-antimonopole density, mean distance, screening length

To appear early November 2011.

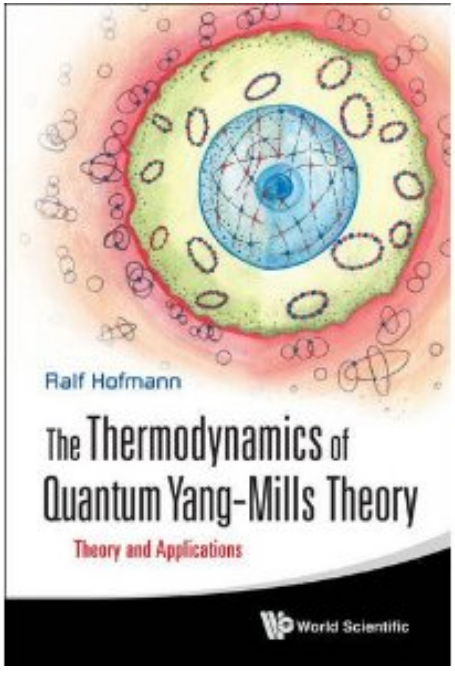

Contains **applications** of $SU(2)_{CMB}$ ($\Lambda \sim 10^{-4}\,\mathrm{eV}$) to:

- black-body anomaly
- contradiction to SM Higgs sector derived from primordial He abundance bounds on freezeout temperature for nucleosynthesis in case $SU(2)_{CMB}$ confirmed
- **U**nexplained **E**xtra**G**alactic **E**mission
- primordial, magnetic seed fields
- stability of cold, dilute H1 clouds in Milky Way

Thank you.